Theoretical Study on Fatigue Damage of Sonic Standing Wave Resonant Drill-String

Changgen Bu [a,*], Jing Xiao [a], Shengyu He [a], Marian Wiercigroch [b,*]

[a] School of Engineering and Technology, China University of Geosciences, Beijing 100083, China

[b] Centre for Applied Dynamics Research, School of Engineering, University of Aberdeen, Aberdeen AB24 3UE, UK

Abstract: To achieve high-speed and undisturbed core drilling, the standing wave vibration of the drill string in a sonic drill is excited by a high-frequency inertial vibrator; the resulting high alternating stress cycle in the drill string can easily cause fatigue damage. In order to minimize the fatigue failure of drill-string at the stage of its design, it is necessary to assess the fatigue damage caused by alternating stress to guide engineering practice. In this paper, based on one-dimensional wave theory, we analyse the standing wave vibration in a drill-string excited by a sonic vibrator, and theoretically prove that the dynamic resonant stress of a drill-string is the key factor influencing the fatigue damage. By using the Palmgren–Miner fatigue damage rule, we establish a theoretical formula for the cumulative fatigue damage of a variable-length standing wave vibration drill string and reveal the fatigue damage mechanism of the variable-length resonant drill string. Furthermore, the effects of sonic drill systems and process parameters on the damage are quantified. It was found that by an appropriate choice of a drill-pipe length, the fatigue damage can reduced whilst the axial stress concentration factor (aSCF) k_σ on threaded connections can significantly it. At the fundamental frequency of the resonant sonic drilling, the maximum fatigue damage point, x_f, is located approximately $l_a/2$ above the drill bit, not exceeding the theoretical sonic standing wave starting length, l_a, and unrelated to the hole depth. This study promotes the theoretical understanding and exploration of variable-length standing wave oscillators.

Keywords: Sonic drill; Cumulative fatigue damage; Variable length drill string; Standing wave resonance; Palmgren–Miner rule; Threaded connection

* Corresponding author.

E-mail address: bucg@cugb.edu.cn(C.Bu), m.wiercigroch@abdn.ac.uk (M. Wiercigroch).

Nomenclature

c	Damping
d_i	Inner diameter of drill string
d_o	Outer diameter of drill string
$f(x,t)$	Distributed load
k_σ	Axial stress concentration factor
l	Total length of drill string
l_a	Theoretical starting length of sonic standing wave
l_b	Length of drill string without fatigue damage
l_0	Maximum length of drill string, not exceeding l_a
m	Material constant
m_e	Static moment of sonic vibrator
n_k	Number of cycles under the stress level σ_{-1k}
$u(x,t)$	Displacement response of drill string
x_f	Maximum fatigue damage point
D	Cumulative fatigue damage
D_k	Fatigue damage under the stress level σ_{-1k}
E	Elastic modulus
N_C	Total number of cycles under the stress level σ_{-1}
N_k	Total number of cycles under the stress level σ_{-1k}
S	Cross-sectional area of drill string
V	Rate of penetration (ROP)
Δl	Length of a single drill pipe
ξ	Damping ratio
ρ	Density
$\lambda_r(x,t)$	Estimated deviation between resonant order dynamic stress and total dynamic stress
$\sigma(x,t)$	Dynamic stress
σ_b	Tensile strength
σ_{-1}	Symmetrical cyclic fatigue limit stress
σ_{-1k}	Stress level
φ_i	Phase angle
ω_i	i^{th} order natural frequency
API	American Petroleum Institute

1. Introduction

For geological drilling and oil drilling, drill string dynamics problems have been widely concerned, the purpose of solving dynamic problems is mostly to improve drilling efficiency and reduce losses caused by drill string failure. Scholars worldwide have focused on the dynamic modelling of drill strings based on simplifications and assessments of downhole interactions and exercises to predict the axial, torsional, and bending vibration (Ghasemloonia et al., 2015; Jansen 1991; Leine et al., 1998; Mihajlović et al., 2007; Vandiver et al., 1990; Yigit and Christoforou 2006; Zhao et al., 2018). In particular, some scholars have employed a reduced-order model to simplify the complex boundary dynamic problem of drill string coupling vibrations (Kapitaniak et al., 2015; Liao et al., 2012; Liu et al., 2014). Drilling tool failures can be caused by various reasons mostly associated with excessive loads and tear and wear of drill-string components. Drilling fluids can help to reduce the problem as was shown by Jiang et al. (2021) by developing a new drilling fluids technology to improve wellbore quality and reduce drill-string wear. Tension, compression, bending, and twisting stresses through the drilling process can also result in drilling tool failures, reduced rates of penetration, increase times to replace failed tools (Albdiry and Almensory 2016). Occurrences of downhole failures of drill-strings disrupt drilling operations, which can result in heavy financial losses due to non- productive time (Zamani et al., 2016). Statistical data indicate that over 50% of drill string failures result from fatigue (Macdonald and Bjune 2007; Moradi and Ranjbar 2009); consequently, the fatigue damage of drill strings is a dynamic problem that has garnered the attention of researchers worldwide.

Recently, ultrasonic standing waves have been used to enhance oil production and Wang et al. (2022) studied the dynamic performance of the foam surface subjected to ultrasonic standing wave fields and developed a novel solution to defoam drilling liquids. Sonic drills also use standing resonant waves to achieve high progression rates and better quality of borehole which is important for sample coring. However, a drill string with standing wave resonance undergoes significant dynamic stress at a specific position. Furthermore, as the length of the drill string increases on extending the drilling hole, this position of the maximum dynamic stress changes. Therefore, the mechanism of fatigue damage in the drill strings of sonic drills should be determined first. Analysing the fatigue damage in a sonic drill string can help reduce drilling accidents and prolong the service life of sonic drill strings.

Fatigue failure is caused by the accumulation of fatigue damage, which eventually reaches the critical value. For almost a century, researchers have proposed many theoretical models to describe the development of cumulative damage (Benkabouche et al., 2015; Fatemi and Yang 1998). In 1924, Palmgren first proposed the linear accumulation hypothesis for fatigue damage. In 1945, Miner (1945) developed this theory and formulated the Palmgren–Miner linear accumulation damage rule (or Miner’s rule). Thereafter, based on experimental research, many novel linear cumulative damage models have been proposed and applied in engineering (Proso et al., 2016; Rahman et al., 1999; Zambrano and Foti 2014; Zhao 2000; Zhu et al., 2011). In addition, the nonlinear damage theory based on multiaxial stress (Benkabouche et al., 2015; Freitas 2017; He et al., 2018; Lin et al., 2016; Lv et al., 2015; Nesládek et al., 2012; Susmel et al., 2005; Zhang et al., 2021; Zhuang et al., 2019) and fracture and damage mechanics (Albdiry and Almensory 2016; Ojanomare et al., 2017; Sun et al., 2020; Xu et al., 2021; Zamani et al., 2016; Zhao et al., 2020; Zhuang et al., 2019) have been developed rapidly. In some cases, multiaxial stress fatigue experiments have indicated that the Palmgren–Miner rule is in good agreement with experimental results (Xia and Yao 2013). In 1956, based on Grover's viewpoint, Corten and Dolan (1956) proposed that cumulative damage is related to loading, and they established the Corten–Dolan cumulative damage theory. Moreover, the modified nonlinear Corten–Dolan model exhibits significantly superior life prediction capability, as compared to its predecessor (Lv et al., 2015; Zhu et al., 2012). Manson (1966) divided the fatigue process into stages of crack formation and crack propagation and established the bilinear cumulative damage theory for different stages by utilising the linear cumulative damage rule. Following the introduction of fracture and damage mechanics, the cumulative damage process was explained from a microscopic perspective. In 1963, Paris and Erdogan (1963) expressed the crack growth law using fracture mechanics; the Paris formula is used to estimate fatigue life and serves as a novel method for investigating the same. Based on the work of Paris, Forman et al., (1997) considered the effect of the fracture toughness of a material on the crack growth rate, improved the Paris formula, and established the Forman model. In 1970, Walker (1970) further considered the influence of the stress ratio on the fatigue crack growth rate and proposed the Walker model. Among these methods, Miner’s rule and the Corten–Dolan model have been widely used in engineering. However, the Corten–Dolan model occasionally yields results with significant errors; this is because the method of determining the Corten–Dolan exponent is often empirical or semi-empirical (Rao et al., 2001; Zhao 2000).

In engineering practice, the fatigue analysis methods vary depending on the forms of stress. Miner's cumulative fatigue damage theory is simple and convenient to use, and its calculation results are in good agreement with the test results for most cases; it can also be used to predict the average fatigue life of engineering structures subjected to random loads (Sun et al., 2014). Therefore, this theory is widely used for predicting the fatigue life of general mechanical parts used in engineering, aircraft engines, skins, hydraulic pipes, and other components (Baek et al., 2008; Chen et al., 2014; Rui et al., 2018; Shi 2014; Zambrano and Foti 2014; Zhao et al., 2020). Rao et al. (2001) emphasized that the Palmgren–Miner rule is the most commonly used theory for predicting the fatigue life of a blade subjected to variable stress amplitudes.

In recent years, scholars have studied the fatigue life of drill strings based on fracture mechanics. Dao and Sellami (2012) obtained the stress intensity factor through finite element analyses. Ojanomare et al. (2017) determined the stress intensity factor of a drill string through a multi-parameter weight function; they substituted the stress intensity factor and the crack growth rate in the relationship to estimate the fatigue life of the drill string. Over 50% of the fatigue failures in drill strings occur at the drill-pipe joint (Chen 1990; Grondin and Kulak 1994; Knight and Brennan 1999; Macdonald and Bjune 2007). Based on analyses of drill pipe failures, Zamani (2016) believed that, under the action of seven influential forces, including complex stress, the drill string undergoes an initial crack and continuously develops fatigue fracture. Bertini et al. (2008) and Santus et al. (2008, 2018) set up a resonant experimental platform and studied the fretting wear of aluminium–steel joints in aluminium alloy drill pipes; they revealed that fretting resulted in the initial crack, nucleation, and fatigue fracture and that the fatigue analysis of the symmetrical cyclic stress in the resonance experiment exhibits clear linear characteristics. Most scholars have investigated the fatigue life of drill strings considering the fields of geological drilling and petroleum drilling engineering, mainly based on the linear fatigue cumulative damage theory. Rahman et al. (1999) believed that the die marks generated on the surface of the drill pipe during the clamping process of the feeding system result in stress concentration and influence the fatigue of the drill string, and they used the stress concentration factor to modify the alternating stress generated by the rotation and bending at dangerous points, and analysed the cumulative fatigue damage of the drill string based on the Miner fatigue cumulative damage theory. Sikal et al. (2008) simulated the drilling trajectory and bending state of a drill string; calculated the asymmetric cyclic stress generated by the torsion, bending, and stretching at a specific position in the drill string during drilling; obtained the symmetric cyclic stress based on the Goodman model; and determined the cumulative fatigue damage at a specific location in the drill string based on the Miner cumulative fatigue damage theory. Zhao et al. (2018) proposed a two-degree-of-freedom nonlinear lumped-mass model that accounted for stick/slip vibrations and Hertzian contact forces, in order to simulate the time-domain responses of whirl on the drill collar; furthermore, the bending cumulative fatigue at the connection was investigated based on the Miner method, and the results indicated that vibration is a major cause of connection fatigue. When using a sonic drill for drilling, the length of the drill string varies as the borehole is extended, and each point in the drill string is subjected to variable-amplitude loads (Bu et al., 2015). When the stress level exceeds the fatigue limit of the drill string material, each cycle causes damage to the drill string. When the cumulative damage reaches a certain critical level, fatigue failure of the drill string occurs. In tests involving asymmetric cyclic loadings of constant and variable-amplitude loads, the frequency of ultrasonic testing has no effect on the fatigue life (Fitzka and Mayer 2016; Mayer et al., 2013). Moreover, the Palmgren–Miner rule affords better life predictions under simple load conditions, as compared to the other approaches (Zhu et al. 2012).

To provide theoretical support for minimizing the fatigue failure of a drill string in engineering practice, based on Palmgren–Miner linear cumulative fatigue damage theory and one-dimensional wave theory, a novel theoretical formula is established to describe the cumulative fatigue damage of a variable-length standing wave vibration drill-string. The formula is obtained by the following process: 1) Establish a sonic excitation drill string system model for determining the dynamic stress of drill strings with different lengths; 2) Identify the dynamic stress that affects the fatigue life of drill strings; 3) Determine the number of stress cycles and the fatigue life under different stress levels; 4) Determine the cumulative fatigue damage. According to the formula, the effects of sonic drill systems and process parameters on the damage are quantified. At the fundamental frequency of the resonant sonic drilling, the maximum fatigue damage point, x_f, is located approximately $l_a/2$ above the drill bit, not exceeding the theoretical sonic standing wave starting length, l_a, and unrelated to the hole depth. Furthermore, through the introduction of axial stress concentration factor (aSCF) k_σ, the theoretical calculation formula of fatigue damage at the joint is established. This research and its results are expected to serve as a theoretical basis for sonic drill designs and production practices, in order to improve the service life of and reduce the risk of fatigue failure in drilling tools.

2. Methodology

Sonic drills mainly employ sonic vibrators to generate a harmonic excitation force in order to drive the high-frequency vibration of the drill string. When the excited drill-string is in the standing wave vibration state, significant alternating stresses are generated in the drill string, which may result in the fatigue or fracture of the drill string. Bu et al. (2015) studied the sonic excitation of drill string vibration and showed that the dynamic stress field of each point in the drill string can be solved via mathematical modelling to obtain an explicit expression; they also reported that the vibration response of each point in the drill string is the superposition of the forced vibration response of the n^{th} mode shapes. For a sonic drill string of a specific length, the response of each order of the forced vibration dynamic stress is a periodic function of the harmonic alternating stress; the Palmgren–Miner cumulative fatigue damage rule can help understand the fatigue of a drill-string excited by a sonic vibrator.

2.1. Fatigue damage of a sonic drill-string

The Palmgren–Miner cumulative fatigue damage theory states that fatigue damage is a linear cumulative process under cyclic loading. When the cumulative damage reaches a critical value, the specimen undergoes fatigue failure. The cumulative fatigue damage *D* can be written as

$$D = \sum D_k = \sum \frac{n_k}{N_k}, \tag{1}$$

where n_k is the number of cycles under the stress level σ_{-1k} ($k = 1, 2, 3\cdots$), N_k is the total number of cycles that the test piece can withstand under the stress level σ_{-1k} (i.e. fatigue life), and D_k is the fatigue damage under the stress level σ_{-1k}. When the stress level is known, the fatigue life of the test piece under this condition can be determined based on the $\sigma - N$ curve. The $\sigma - N$ curve obeys the Basquin model (Ciavarella et al., 2017). The expression can be written as

$$\sigma_{-1k}^{m} N_k = \sigma_{-1}^{m} N_C \tag{2}$$

where *m* is the material constant, σ_{-1} is the symmetrical cyclic fatigue limit, and N_c is the fatigue life corresponding to σ_{-1}, generally assumed as $N_C = 10^7$. The $\sigma - N$ curve of the test piece is obtained from a fatigue test using standard specimens of the same material (Liu et al., 2016; Lin et al., 2015). According to Lin et al. (2015), in the fatigue performance tests of the commonly used S135 and G105 materials, the material constants of the drill pipes are obtained when the survival rate is 99%. S135 and G105 high-strength alloy steel API drill pipes are selected for sonic drilling. The drill pipe material constants are listed in Table 1.

Table 1. Material constants of drill pipe (ISO11961:2008; Lin et al., 2015).

Drill pipe material	Fatigue limit $\sigma_{-1}\,(MPa)$	Tensile strength $\sigma_b\,(MPa)$	Material constant m	Density $\rho\,(kg/m^3)$	Elastic modulus $E\,(Pa)$
S135	527.37	1000	16.53	7850	$2.06e^{11}$
G105	435.62	793	9.77	7850	$2.06e^{11}$

During sonic drilling, the length of the drill string changes continuously as the borehole extends, and the stress level in the drill string also varies accordingly. Based on the Palmgren–Miner cumulative fatigue damage rule, after selecting the drill pipe material, to determine the fatigue damage in a sonic drill string at a specific location, the stress level and the number of stress cycles must be determined for different drill string lengths. The fatigue life at this stress level can be obtained by Eq. (2), which can then be used in Eq. (1) to determine the fatigue damage at a specific position of the drill string.

2.2. Modelling the sonic excitation drill string system

A sonic vibrator is installed at the top of a sonic drill; this vibrator is used to excite the drill string vibrations. Certain large sonic drills are also equipped with a top drive gyrator to rotate the drill string for achieving rotary sonic drilling. The top drive gyrator and the sonic vibrator are isolated by air springs; thus, they do not participate in the excitation of the sonic vibrator to cause drill string resonance (Xiao et al., 2019). When the sonic drill is operated in a saturated stratum or with limited drilling fluid, the vibration and deformation result in a rapid increase in the water pressure in the voids of the thin layer of soil in contact with the drill string; this causes the soil to liquefy into a viscous fluid with a dynamic state, and the shear strength and stiffness approach zero (Barrow 1994). Therefore, only the influence of the viscous fluid damping on the drill string vibrations is considered; the influence of the gravitational field and the lateral effects are neglected. Thus, under the steady-state excitation of the sonic vibrator, a drill string model is established as shown in Fig. 1.

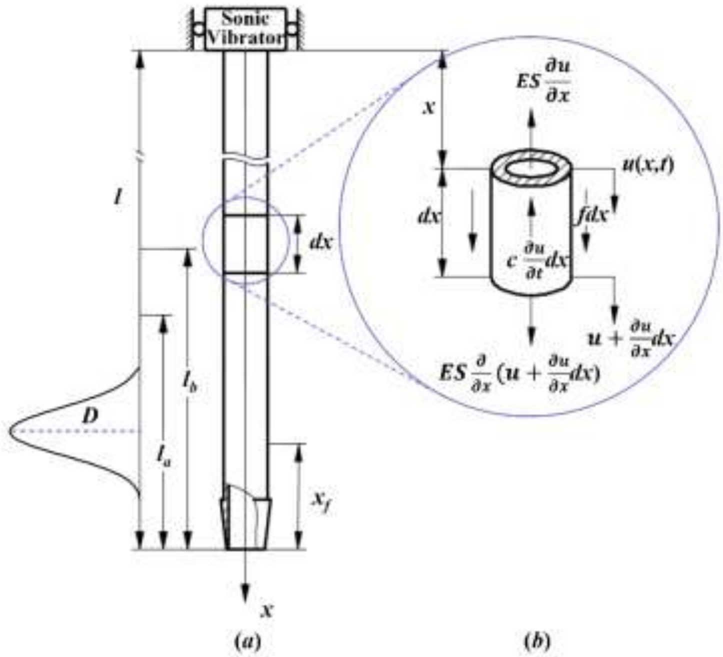

Fig. 1. Model of the sonic excitation drill string system. (a) Schematic diagram of an example of cumulative fatigue damage of the G105 drill pipes. Under the condition that the excitation frequency is 200 Hz, the position of the maximum fatigue damage point of the axial standing wave vibration of the drill string of length l is around $l_a/2$ above the drill bit. (b) Schematic diagram of displacement, stress and external load of drill string micro-element in the axial direction.

The differential equation of the longitudinal vibration of a uniform cross-section sonic drill string subjected to the distributed load $f(x,t)$ is

$$\rho S\frac{\partial^2 u}{\partial t^2}+c\frac{\partial u}{\partial t}-ES\frac{\partial^2 u}{\partial x^2}=f(x,t) \tag{3}$$

where the longitudinally distributed load generated by the sonic vibrator is $f(x,t)=m_e\omega^2\sin\omega t\ \delta(x)=\begin{cases} m_e\omega^2\sin\omega t\,, & x=0 \\ 0\,, & x\neq 0\end{cases}$, and the boundary conditions of the sonic drill string system can be written as Eq. (4).

$$\frac{\partial u(0,t)}{\partial x}=\frac{\partial u(l,t)}{\partial x}=0 \tag{4}$$

Using the method of separation of variables, the steady-state solution of the forced vibration displacement response of the drill string is obtained (Sun et al., 2017):

$$u(x,t)=\frac{2m_e\omega^2}{\rho Sl}\sum_{i=0}^{\infty}\frac{\sin(\omega t-\varphi_i)}{\sqrt{(\omega_i^2-\omega^2)^2+(2\zeta_i\omega_i\omega)^2}}\cos\frac{i\pi x}{l} \tag{5}$$

where the natural frequency of each order of the drill string is $\omega_i=i\pi\sqrt{E/\rho}\big/l$ ($i=0,1,2\cdots$). When adjusting the angular frequency ω of the sonic vibrator to approach the natural frequency of the drill string ω_i, the sonic drill is in a state of standing wave resonance. The phase angle $\varphi_i = \arctan\dfrac{2\zeta_i\omega_i\omega}{\omega_i^2-\omega^2} \to \pi/2$, and ζ_i is the mode shape damping ratio. In engineering, it is typically assumed that the damping ratio of each mode shape is the same (Wen et al., 2009); therefore, $\zeta = \zeta_i$ is assumed in this study.

The strain field $\varepsilon(x,t) = \dfrac{\partial u(x,t)}{\partial x}$ is obtained from the partial derivative of the displacement field with respect to x, and the steady-state solution of the dynamic stress response of each point in the drill string is obtained as Eq. (6).

$$\sigma(x,t) = E\varepsilon(x,t) = -\frac{2\pi E m_e \omega^2}{\rho S l^2}\sum_{i=0}^{\infty}\frac{i\sin(\omega t-\varphi_i)}{\sqrt{(\omega_i^2-\omega^2)^2+(2\zeta\omega_i\omega)^2}}\sin\frac{i\pi x}{l} \tag{6}$$

Eq. (6) expresses the dynamic stress at any position in the drill string at any time. However, the dynamic stress response of a drill string is the superposition of the forced vibration dynamic stress of each mode. Thus, the stress level at a specific location cannot be obtained directly from Eq. (6); further analyses are needed to determine the dynamic stress that causes fatigue damage in drill strings.

2.3. Stress field analysis of sonic standing wave vibration drill string

In sonic drilling, first-, second-, or third-order frequency vibration drilling is generally used to ensure reliable and efficient drilling. Thus, this study focuses on the fatigue damage of a low-order resonance drill string. The technical parameters of the sonic vibrator and drill pipe are listed in Table 2.

Table 2. Technical parameters of sonic vibrator and drill pipe (ISO11961:2008; Sun et al., 2017).

Total static moment of sonic vibrator m_e	Drill-string inner/outer diameter d_i / d_o	Drill-string cross-sectional area S
0.126 kg · m	92.46/114.3 mm	3.547e^{-3} m^2

When the drill string undergoes the r^{th}-order resonance, the angular frequency of the sonic vibrator ω approaches the r^{th}-order natural frequency, ω_r. From Eq. (6), the dynamic stress, $\sigma_{ri}(x,t)$, at each point in the drill string caused by the i^{th}-order forced vibration is expressed as Eq. (7).

$$\sigma_{ri}(x,t) = -\frac{2\pi E m_e}{\rho S l^2}\cdot\frac{i\cdot\sin(\omega_r t-\varphi_i)}{\sqrt{[(\frac{\omega_i}{\omega_r})^2-1]^2+(2\zeta\cdot\frac{\omega_i}{\omega_r})^2}}\cdot\sin\frac{i\pi x}{l} \tag{7}$$

Substituting the ratio of the i^{th}-order to the r^{th}-order natural frequency into Eq. (7), the dynamic stress can be obtained by simplification as Eq. (8).

$$\sigma_{ri}(x,t) = -\frac{2i}{\sqrt{[(\frac{i}{r})^2-1]^2+(2\zeta\cdot\frac{i}{r})^2}}\cdot\frac{\pi E m_e}{\rho S l^2}\cdot\sin\frac{i\pi x}{l}\cdot\sin(\omega_r t-\varphi_i) \tag{8}$$

From Eq. (8), for a specific drill string length *l*, when the sonic drill is in r^{th}-order resonance during drilling, the maximum dynamic stress amplitude generated by the i^{th}-order of the forced vibration in the drill string is

$$\sigma_{ri\max} = \frac{2i}{\sqrt{[(\frac{i}{r})^2-1]^2+(2\zeta\cdot\frac{i}{r})^2}}\cdot\frac{\pi E m_e}{\rho S l^2} \tag{9}$$

Specifically, when $i = r$, Eq.(9) can be simplified as Eq. (10).

$$\sigma_{rr\max} = \frac{r}{\zeta}\cdot\frac{\pi E m_e}{\rho S l^2} \tag{10}$$

To study the effect of the dynamic stress generated by different orders of the forced vibration on the fatigue life of the drill string, we first compare the maximum dynamic stress amplitude of the i^{th}- order forced vibration and the r^{th}-order resonance, obtained as Eq. (11).

$$\frac{\sigma_{ri\max}}{\sigma_{rr\max}} = \frac{2\zeta\cdot\frac{i}{r}}{\sqrt{[(\frac{i}{r})^2-1]^2+(2\zeta\cdot\frac{i}{r})^2}} \tag{11}$$

From Eq. (11), the maximum stress ratio $\sigma_{ri\max}/\sigma_{rr\max}$ generated between the i^{th}-order forced vibration and the r^{th}-order resonance is a function of the ratio i/r. When $i = r$, the value of $\sigma_{ri\max}/\sigma_{rr\max}$ is 1. The maximum stress ratio $\sigma_{ri\max}/\sigma_{rr\max}$ generated between the $(r\text{-}1)^{\text{th}}$ or the $(r\text{+}1)^{\text{th}}$-order forced vibration and the r^{th}-order resonance is the largest when $i \neq r$. Investigating the maximum dynamic stress of the $(r\text{-}1)^{\text{th}}$-order and $(r\text{+}1)^{\text{th}}$-order forced vibration and the r^{th}-order resonance yields Eq. (12).

$$\begin{cases} \dfrac{\sigma_{(r+1)\max}}{\sigma_{r\max}} = \dfrac{2r(r+1)\zeta}{\sqrt{[(r+1)^2-r^2)]^2+[2r(r+1)\zeta]^2}} < \dfrac{2r(r+1)\zeta}{\sqrt{[(r+1)^2-r^2)]^2}} = \dfrac{2r(r+1)\zeta}{r+1+r} = \dfrac{2r\zeta}{1+\dfrac{r}{r+1}} < 2r\zeta \quad ,r\geq 1 \\ \dfrac{\sigma_{(r-1)\max}}{\sigma_{r\max}} = \dfrac{2r(r-1)\zeta}{\sqrt{[r^2-(r-1)^2)]^2+[2r(r-1)\zeta]^2}} < \dfrac{2r(r-1)\zeta}{\sqrt{[r^2-(r-1)^2)]^2}} = \dfrac{2(r-1)r\zeta}{r-1+r} = \dfrac{2r\zeta}{1+\dfrac{r}{(r-1)}} < 2r\zeta \quad ,r>1 \end{cases} \tag{12}$$

Therefore, the range of values of the ratio of the maximum stress amplitude of the i^{th}-order non-resonant forced vibration to the maximum stress amplitude of the r^{th}-order resonance is expressed as Eq. (13).

$$\frac{\sigma_{ri\max}}{\sigma_{rr\max}} < 2r\zeta \quad , \quad i\neq r \tag{13}$$

When the sonic drill undergoes standing wave resonance, its resonance order *r* is generally the first or second order and not greater than the third order. For the sonic drill, when a lower-order mode is used to drill in a saturated stratum or with limited circulating fluid, it can be regarded as a small damping system ($0 \le \zeta_i \le 0.2$). When the ratio of the maximum stress value of the other non-resonant forced vibrations to the maximum stress value of the resonance order is less than $2r\zeta$, it can be considered that the dynamic stress in the drill string is mainly generated by the resonance order.

Furthermore, to analyse the contribution of the dynamic stress of the resonant order to the total dynamic stress in the drill string, we consider the effects of the stress amplitude and phase difference. In the case of resonance, the total stress and the resonant order stress at each point of the drill string can be obtained from Eq. (6) and Eq. (7), as shown in Fig. 2.

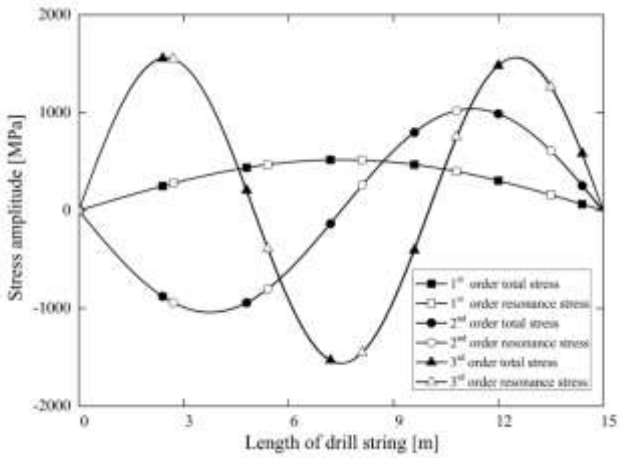

Fig. 2. Total stress and resonance stress amplitudes for the first three orders at each point of the G105 drill string with a length of 15 m (under the technical parameters of Table 2) and damping ratio $\zeta = 0.025$.

As can be seen from Fig. 2, the amplitudes of the dynamic stress of the resonant order and the total dynamic stress in the drill string are highly consistent. The fatigue damage of a drill string is primarily caused by the dynamic stress exceeding the symmetrical cyclic fatigue limit. Therefore, it is necessary to accurately analyse the amplitude deviation between the dynamic stress in the drill string and the dynamic stress of the resonant order that exceeds the symmetrical cyclic fatigue limit. The estimated deviation between the dynamic stress of the resonant order and the total dynamic stress in the drill string can be expressed as Eq. (14).

$$\lambda_r(x,t) = \left| \frac{\sigma_{rr}(x,t) - \sigma(x,t)}{\sigma(x,t)} \right| \tag{14}$$

In the case of the G105 drill string, which has a length of 15 m and a damping ratio of

$\zeta = 0.025$, as shown in Fig. 2, the maximum deviation between the dynamic stress of the first-order resonance and the total stress of the drill string is 1.2‰. The maximum deviation between the dynamic stress of the second-order resonance and the total stress of the drill string is 8.5‰. Moreover, the maximum deviation between the dynamic stress of the third-order resonance and the total stress of the drill string is 3.8%. Notably, the deviation between the dynamic stress of the first-order resonance and the total stress of the drill string is the smallest. As the driving order increases, the deviation gradually increases to a maximum deviation of less than 5%.

Thus, for low-frequency resonant drilling using a sonic drilling rig, when analysing the effects of different orders of dynamic stress in the drill string on the fatigue life, it can be considered that the fatigue damage of the drill string is caused by the resonant order dynamic stress; hence, we only need to account for the fatigue damage at each point in the drill string under the dynamic stress of the resonant order.

Based on the number of stress cycles and the fatigue life of a drill string under different stress levels, we establish a standing wave vibration fatigue damage model for a sonic drill string, in order to determine the cumulative fatigue damage during sonic drilling.

2.4. Characteristic analysis of fatigue damage of sonic drill string

To conveniently model the fatigue damage during sonic drilling, we first analyse the internal stress of the drill string that causes fatigue damage. The upper frequency of the sonic vibrator is limited by its mechanical structure; this frequency generally does not exceed 200 Hz. In other words, the maximum excitation frequency of the sonic vibrator $f_{\max} \le 200\ \mathrm{Hz}$. To generate the r^{th}-order resonance in the drill string, the natural frequency of the drill string should satisfy $f_i \le f_{\max}$. The sonic vibrator can provide the corresponding driving frequency to induce a sonic resonant standing wave in the drill string. Accordingly, the length *l* of the drill string is defined as the theoretical starting length l_a of the standing sonic wave vibration, expressed as Eq. (15).

$$l_a = \frac{r}{2 f_{\max}} \sqrt{\frac{E}{\rho}} \tag{15}$$

From Eq. (15), the theoretical starting length of the r^{th}-order resonant standing wave is $l_a = \frac{r}{2 f_{\max}} \sqrt{\frac{E}{\rho}}$. In the case of a steel alloy drill pipe, when the maximum frequency of the sonic vibrator is $f_{\max} = 200\ \mathrm{Hz}$, the initial length of the drill string of the first-order resonant standing wave is $l_a = 12.8\,\mathrm{m}$.

When the maximum dynamic stress of the drill string $\sigma_{rr\max} \le \sigma_{-1}$, the length of the drill string, without fatigue damage caused by the resonant standing wave l_b, is obtained from Eq. (10), as shown in Eq. (16).

$$l_b = \sqrt{\frac{\pi r m_e}{\zeta \sigma_{-1} S}} \cdot \sqrt{\frac{E}{\rho}} \tag{16}$$

In the case of the G105 drill pipe, the damping ratio $\zeta = 0.025$. From Eq. (16), the length of the first-order standing wave resonant drill string without fatigue damage is $l_b = 16.4\,\mathrm{m}$.

When the standing wave resonant drilling is commenced, the maximum dynamic stress in the drill string is $\sigma_{rr\max} \le \sigma_{-1}$. At this time, $l_a \ge l_b$, and no fatigue damage occurs at any point on the drill string during drilling. The analysis shows that the range of fatigue damage in the drill string during standing wave drilling is $l_a \le l \le l_b$.

In the sonic drilling process, the drill string is short. Thus, the natural frequency of the drill string is high at the start of drilling and the driving frequency of the sonic vibrator cannot induce resonance in the drill string. Therefore, the drill string penetrates the soil in a non-resonant form of the travelling wave; in this case, the internal stress amplitude of the drill string can still be obtained using Eq. (6). As the drilling depth increases, $l \ge l_a$ is satisfied, and the resonant standing wave is adopted for drilling. At this time, the internal stress amplitude of the drill string can be approximated from the dynamic stress amplitude of the resonant order, given by Eq. (10). Assuming that the sonic drill commences the standing wave drilling at the maximum driving frequency of 200 Hz, the relationship curve between the dynamic stress amplitude and the length of the drill string can be obtained considering the non-resonant forced vibration and/or the resonant standing wave, as shown in Fig. 3.

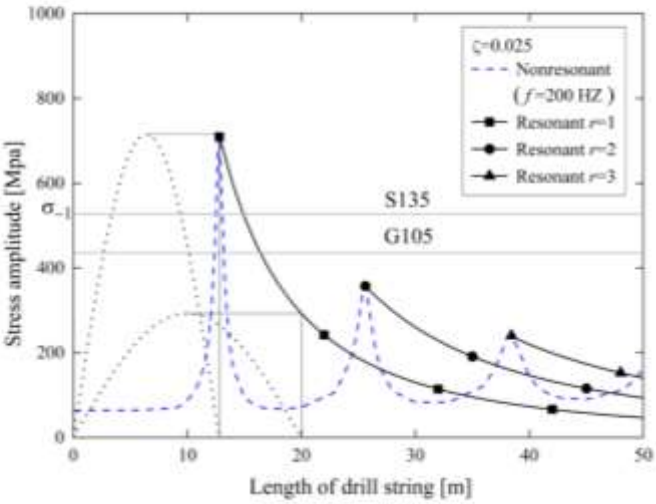

Fig. 3. Relationship between the dynamic stress amplitude of the drill string and drill string length during sonic drilling. The blue dashed line denotes the maximum dynamic stress under non-resonant forced vibration driven by 200 Hz; the black solid line indicates the maximum dynamic stress under the resonant standing wave. The dotted lines represent the maximum dynamic stress at each point of the drill strings with specific lengths of 12.8 m and 20 m, whereas the grey lines denote the fatigue limits of S135 and G105.

If the vibrator drives the sonic drilling at 200 Hz throughout the drilling process, the maximum dynamic stress in the drill string can be obtained from Eq. (6), as indicated by the blue dashed line in Fig. 3. It is observed that the maximum dynamic stress is relatively low at the start of drilling. With an increase in the length of the drill string, when the driving frequency approaches the first-order natural frequency, the dynamic stress in the drill string is redistributed rapidly, and the maximum dynamic stress in the drill string also increases rapidly. If the original driving frequency is retained, the internal dynamic stress amplitude decreases rapidly. When approaching the second- and third-order natural frequencies, the amplitude of the internal stress is redistributed rapidly. If the original driving frequency is maintained, the amplitude of the internal dynamic stress decreases rapidly.

To improve drilling efficiency, when the length of the drill string satisfies Eq. (15), the frequency of the sonic vibrator is continuously adjusted to approach the natural frequency of the variable-length drill string, such that the drill string resonates and the drill bit attains a greater amplitude and impact velocity. The dynamic stress amplitude at each point of the drill string resonance order can be obtained using Eq. (8). Considering the first-order resonance as an example, as shown in Fig. 3, the black dotted line indicates the amplitude of the stress field in the drill string of a specific length; the maximum dynamic stress amplitude in the drill string occurs at the midpoint (i.e., the stationary point). As the borehole is extended, the dynamic stress amplitude at each point of the drill string decreases. When the internal stress amplitude of the drill string is lower than the symmetric cyclic fatigue limit, the drill string no longer suffers stress damage. The maximum dynamic stress amplitude in the drill string can be obtained using Eq. (10), as represented by the black solid line in Fig. 3.

After reaching a certain depth during drilling, in terms of the working capacity of the equipment, the first-order resonance drilling can be continued or the vibrator frequency can be adjusted such that the drill string moves from the first-order resonance to the second or third order. At this point, the internal stress of the drill string is redistributed. If the internal dynamic stress of the drill string exceeds the symmetrical cyclic fatigue limit again, it continues to cause fatigue damage to the drill string. However, if the internal dynamic stress of the drill string remains lower than the symmetrical cyclic fatigue limit after the redistribution, no fatigue damage is caused to the drill string. As shown in Fig. 3, considering S135 and G105 as the drill pipe materials and a damping ratio of $\zeta = 0.025$, the second- and third-order standing wave resonant drilling no longer causes fatigue damage.

The dynamic stress in the drill string is rapidly redistributed when moving from the travelling wave drilling to the standing wave resonant drilling. Therefore, when analysing the fatigue damage in the drill string, we only need to calculate the fatigue damage of the drill string in the standing wave resonance state.

2.5. Mathematical modelling of the cumulative fatigue damage of the sonic drill string

Based on the analysis, during the r^{th}-order standing wave vibration drilling, the influence of other non-resonant forced vibrations on the dynamic stress in the drill string can be neglected. Thus, only the effect of the dynamic stress of the resonant order on the fatigue life of the drill string needs to be considered. Accordingly, for a specific drill string length *l*, the dynamic stress at each point in the drill string can be expressed as Eq. (17).

$$\sigma(x,t) = \sigma_{rr}(x,t) = -\frac{r}{\zeta} \cdot \frac{\pi E m_e}{\rho S l^2} \sin(\frac{r\pi x}{l}) \cdot \sin(\omega_r t - \varphi_r) \tag{17}$$

In sonic drilling, the length of the drill string does not increase continuously. Once the drill pipe length specification Δl is selected, the length of the drill string is increased by integral multiples of Δl. Owing to the constantly changing length of the drill string, the position of a specific point on the drill string, relative to the drill bit, is fixed. Therefore, for convenience, in this study, we analysed the fatigue damage of the drill string at a distance of x_f above the bit for a specific length of the drill string, as shown in Fig. 1; the abscissa $x = l - x_f$, corresponding to the point x_f above the bit, is substituted into Eq. (17). The corresponding dynamic stress at this point is expressed as Eq. (18).

$$\sigma(x,t) = \sigma(l - x_f, t) = -\frac{r}{\zeta} \cdot \frac{\pi E m_e}{\rho S l^2} \sin(r\pi - \frac{r\pi x_f}{l}) \cdot \sin(\omega_r t - \varphi_r) \tag{18}$$

When the length of the drill string is $l \geq l_a$, the frequency of the sonic vibrator is adjusted such that the drill string produces resonant standing waves. If the dynamic stress generated in the drill string exceeds the fatigue limit, it will result in fatigue damage.

Before drilling without the resonant standing wave, the maximum length of the drill string l_0 is an integral multiple of the length of the drill pipe, and it does not exceed the theoretical starting length l_a of the resonant standing wave, $l_0 \leq l_a$. When one drill pipe is added to the drill string, standing wave vibration occurs. With the extension of the borehole, on adding k drill pipes, the length of the drill string is expressed as Eq. (19).

$$l = l_0 + k\Delta l \tag{19}$$

Accordingly, from Eq. (18), it is known that the fatigue stress amplitude σ_{-1k} at the distance x_f above the drill bit is given by Eq. (20).

$$\sigma_{-1k} = \frac{r}{\zeta} \cdot \frac{\pi E m_e}{\rho S (l_0 + k\Delta l)^2} \sin\left(\frac{r \cdot \pi \cdot x_f}{l_0 + k\Delta l}\right) \tag{20}$$

where $k = 1,2,3\cdots$. Based on the stress–life ($\sigma - N$) curve of the materials, it is observed from Eq. (2) that the amplitude of the dynamic stress σ_{-1k} exceeds the fatigue limit σ_{-1} of the drill pipe materials; the corresponding number of total stress cycles N_k is obtained as Eq. (21).

$$N_k = N_c \cdot \left(\frac{\sigma_{-1}}{\sigma_{-1k}}\right)^m \tag{21}$$

If the rate of penetration (ROP) in sonic drilling is V, the time required for drilling a single drill pipe length Δl is $\Delta t = \Delta l / V$. For a specific length of the drill string l_k, the number of stress cycles n_k at the point x_f above the drill bit is given by Eq. (22).

$$n_k = \frac{\omega_r}{2\pi} \cdot \Delta t = \frac{r\Delta l}{2V\left(l_0 + k\Delta l\right)} \cdot \sqrt{\frac{E}{\rho}} \tag{22}$$

After determining the number of fatigue cycles N_k and the number of stress cycles n_k corresponding to the stress level at the point x_f above the drill bit, by substituting Eqs. (20), (21), and (22) into Eq. (1), the cumulative fatigue damage during the r^{th}-order standing wave resonant drilling at this point can be expressed as Eq. (23).

$$D=\sum\frac{n_k}{N_k}=\frac{\pi^m r^{m+1}}{2N_C(\sigma_{-1})^m}\cdot\left(\sqrt{\frac{E}{\rho}}\right)^{2m+1}\cdot\left(\frac{m_e}{S}\right)^m\cdot\frac{1}{V\zeta^m}\cdot\sum_{k=1}^{k_{\max}}\left[\frac{\Delta l}{(l_0+k\Delta l)^{2m+1}}\cdot\sin^m\left(\frac{r\pi x_f}{l_0+k\Delta l}\right)\right] \tag{23}$$

where $k_{\max}$ is the largest integer not exceeding $(l_b-l_0)/\Delta l$. Throughout the sonic drilling process, once the standing wave resonant drilling is commenced, fatigue damage occurs only when the stress level at the point x_f above the drill bit is σ_{-1k} > σ_{-1}, and the length of the drill string undergoing fatigue damage at the point x_f does not exceed the interval $l_a \le l_0+k\Delta l \le l_b$.

From Eq. (23), the cumulative fatigue damage caused by the r^{th} standing wave vibration at the point x_f is related to the technical parameters of the sonic drilling rig system (i.e. the total static moment m_e of the sonic vibrator, length of the drill pipe Δl, and cross-sectional area *S*), material parameters of the drill pipe (i.e. elastic modulus E, density of the drill string ρ, material constant of the drill pipe, and symmetric cyclic fatigue limit), construction parameters (i.e., the ROP and damping ratio), and other conditions.

Furthermore, to analyse the cumulative fatigue damage during sonic drilling, a method for evaluating the fatigue damage of the sonic drill should be established based on the specific technical parameters and construction conditions of sonic drilling. The cumulative fatigue damage at any point in the drill string can be determined using Eq. (23). It is only necessary to calculate the cumulative fatigue damage when the stress level at the distance x_f above the bit exceeds the fatigue limit. If the stress level at x_f does not exceed the fatigue limit factor throughout the sonic drilling, no fatigue damage occurs at this position. Eq. (23) can be quickly solved using MATLAB, a numerical analysis software; the flow chart of this calculation is presented in Fig. 4.

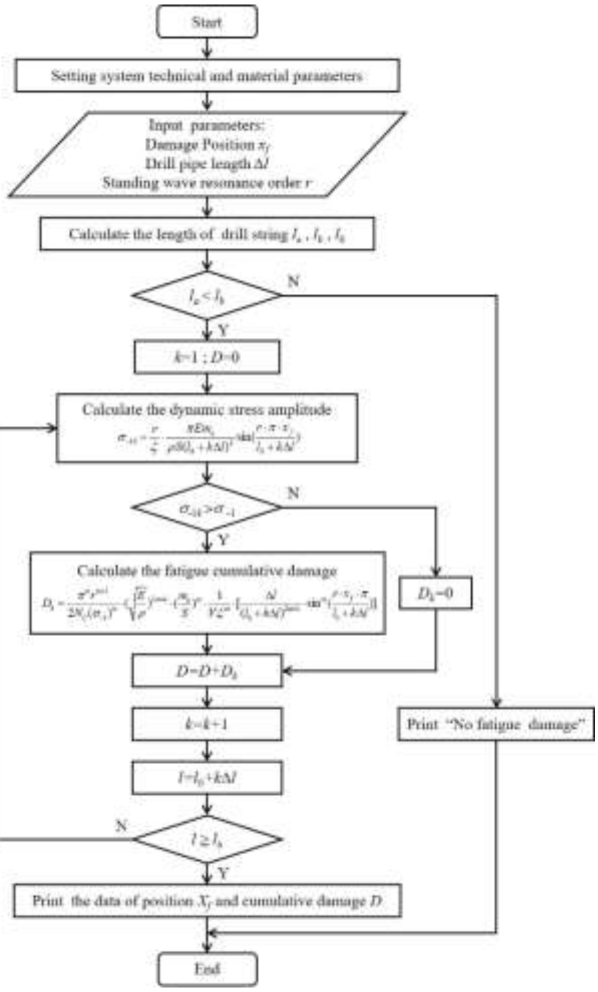

Fig. 4. Flow chart for calculating the cumulative fatigue damage in sonic drill strings. First, determine whether fatigue damage will occur based on the equipment's technical parameters. If so, the total damage value in the whole drilling process can be calculated according to the damage calculation formula and the steps in the figure.

In this study, the cumulative fatigue damage modelling is aimed at a certain order of standing wave resonant drilling. In actual sonic drilling, the first-order resonance is usually used to drill up to a certain depth; this is followed by higher-order resonant drilling in order to improve the drilling efficiency. Accordingly, if the stress level after the redistribution in the drill string exceeds the fatigue limit, the cumulative fatigue damage must be calculated continuously. Based on the initial cumulative damage, the newly generated fatigue damage is calculated to obtain the cumulative fatigue damage. Fig. 4 explains the calculation method employed.

3. Results and discussion

The fatigue damage of the sonic drill string is related to the technical parameters of the sonic drill, the drill pipe material, the length of the drill pipe, construction parameters, and the theoretical starting length of the standing wave resonant drill string. In addition, the technical parameters of the sonic drill, such as the total static moment of the sonic vibrator and the cross-sectional area of the drill string, have a significant influence on the fatigue damage of the drill string, which is directly proportional to the *m*-power of the total static moment of the sonic vibrator and inversely proportional to the *m*-power of the cross-sectional area of the drill string (*m* is the material constant of the drill pipe). Under the premise of ensuring the amplitude and speed of the drill bit in order to achieve high-efficiency dynamic crushing of rocks, reducing the total static moment or increasing the cross-sectional area of the drill pipe can reduce the fatigue damage of the sonic drill string.

In drilling practice, the drill string is typically stimulated to enter the first-order standing wave resonance mode for sonic drilling. Considering first-order standing wave resonant full-hole drilling, this study analyses the influence of the drill pipe material, construction parameters, and length of the drill pipe on the fatigue damage of the sonic drill string in the actual drilling process.

3.1. Verification of the model

The experimental data of G105 material fatigue limit is given in the literature cited in this paper (Lin et al., 2015). For example, four fatigue life datasets ranging from 3.18e5 to 4.67e5 were obtained for whiles symmetrical cyclic stress of 600 MPa was applied, and the fatigue life curve is obtained by using the experimental parameters. G105 material's fatigue stress limit $\sigma_{-1} = 435.62\ \text{MPa}$ and material constant *m*=9.77. Basquin model $\sigma_{-1k}^{m} N_k = \sigma_{-1}^{m} N_C$ is used to predict the material fatigue life under specific stress, as shown in the following Table 3.

Table 3. Comparison of experimental data and theoretical data

Load Stress (MPa)	Experimental fatigue life（Lin et al., 2015）	Model predicted fatigue life	Dynamic stress amplitude of 14m drill string (MPa)	Fatigue life of drill string calculated by Eq. (23)
600	3.18e5, 3.63e5, 4.23e5, 4.67e5	4.38e5	597.76	4.55e5

Assuming a very low ROP when drilling in hard formations and drilling 1 m, the drilling speed is V=4e-4 m/s, and the total length of the new drill string connected by the vibrator is *l*=14 m. According to Eq. (18), the standing wave resonance stress amplitude is 597.76 MPa. In this case, we tested the drill-string fatigue damage, and according to Eqs (22) and (23), the number of stress cycles for fatigue fracture of the drill-string is 4.55e5. The calculation result of Eq. (23) is almost consistent with the model prediction and within the range of experimental data. This shows that it is correct to set up the fatigue calculation theory of standing wave resonance drill-string based on Miner's rule and Basquin model in this paper.

3.2. Effect of drill pipe material on cumulative fatigue damage

S135 and G105 alloy steels, which have the same wave velocity and different grades, are commonly used in drill pipes. These materials directly affect the symmetrical cyclic fatigue limit and material constant. Based on Eq. (23), the fatigue damage of a drill pipe is proportional to the *m*-power of the ratio $\left(m_e / \zeta S \sigma_{-1}\right)$ of the total static moment, the fatigue limit, the cross-sectional area, the damping ratio, and the (2*m*+1)-power of the wave velocity $\sqrt{E/\rho}$. Clearly, it is impossible to judge the influence of the material grade on fatigue damage simply based on the fatigue limit. From Table 1, the fatigue limit and material constant of high-strength drill pipes are higher than those of low-strength drill pipes. For the S135 and G105 high-strength alloy steel drill pipes commonly used in API, the total cumulative fatigue damage to each point in the drill string is calculated using Eq. (23). The influence of the material strength on fatigue damage is illustrated in Fig. 5.

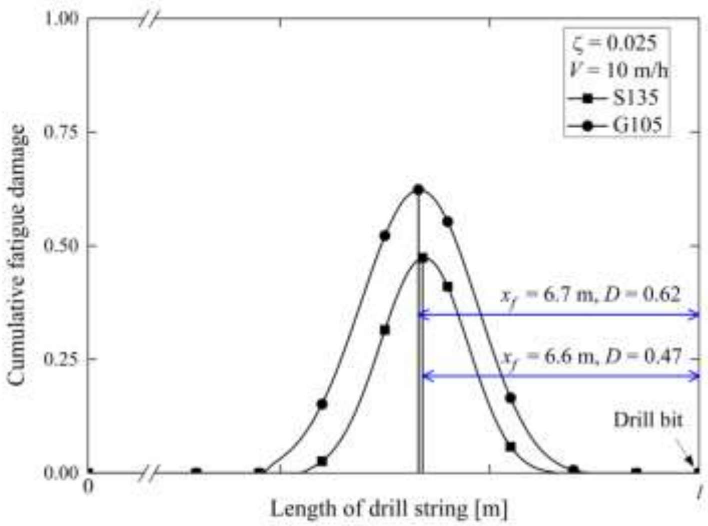

Fig. 5. Cumulative fatigue damage of the S135 and G105 drill pipes under the drilling conditions $V = 10 \text{ m h}^{-1}$, $\zeta = 0.025$, and $\Delta l = 0.1 \text{ m}$. The distance between the maximum damage point and the drill bit is indicated by the blue line.

Under the same ROP of $V = 10 \text{ m h}^{-1}$ and damping ratio $\zeta = 0.025$, the length of the drill string increases almost continuously for the drill pipe length $\Delta l = 0.1 \text{ m}$. The maximum fatigue damage point for the G105 alloy steel drill string is located at a distance of $x_f = 6.7 \text{ m}$ above the drill bit, and the maximum cumulative fatigue damage is $D = 0.62$. The maximum fatigue damage point for the S135 alloy steel drill pipe is located at a distance of $x_f = 6.6$ m above the drill bit, and the maximum cumulative fatigue damage is $D = 0.47$. The fatigue damage of the S135 drill pipe with a higher grade is 31.9% lower than that of the G105 drill pipe. Therefore, if the economic cost is considered, it is advisable to choose high-strength alloy steel drill pipes to prolong the fatigue life under high stress cycles.

Fatigue damage in the drill string is distributed mainly within the range of the theoretical starting length of the resonant standing waves above the drill bit. The maximum damage point x_f of the drill string is located approximately $l_a/2$ above the drill bit, and it does not exceed l_a.

3.3. Effect of construction parameters on cumulative fatigue damage

The construction parameters for sonic drilling include the ROP and the damping ratio of the formation. The effects of the same damping ratio with different ROPs and different damping ratios with the same ROP on the drill string fatigue damage are studied and shown in Fig. 6.

Under a system damping ratio of $\zeta = 0.025$, when the ROP is $V = 10$ m h^{-1}, the maximum damage point of the G105 drill string is located at a distance of $x_f = 6.7$ m above the drill bit, and the maximum fatigue damage is $D = 0.62$. When the ROP is $V = 20$ m h^{-1}, the maximum damage point of the G105 drill string is located at a distance of $x_f = 6.7$ m above the drill bit, and the maximum fatigue damage is $D = 0.31$. The total fatigue damage is reduced by 50% when the ROP is doubled. The maximum fatigue damage is inversely proportional to the ROP. Thus, increasing the ROP appropriately can shorten the drilling time at high stress levels, thereby reducing the number of stress cycles and the cumulative fatigue damage. The maximum damage point x_f of the drill string is located approximately $l_a/2$ above the drill bit.

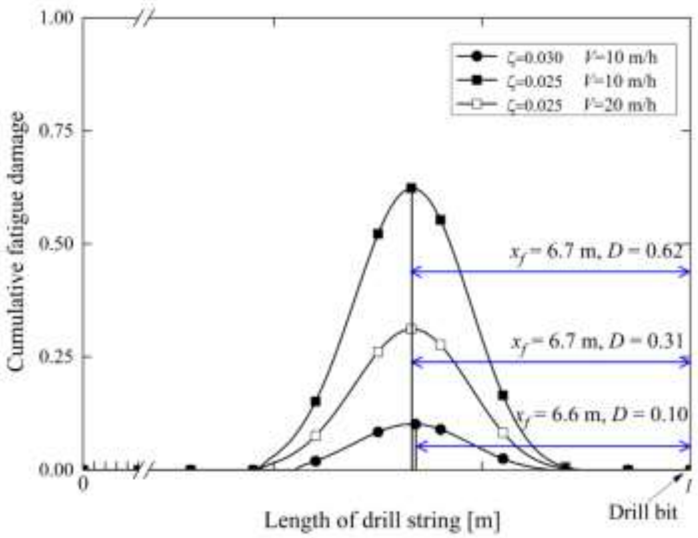

Fig. 6. Influence of construction parameters on the fatigue damage of the drill string (G105 drill pipe, $\Delta l = 0.1$ m); three drilling conditions were considered: $V = 10$ m h^{-1} and $\zeta = 0.025$; $V = 20$ m h^{-1} and $\zeta = 0.025$; and $V = 10$ m h^{-1} and $\zeta = 0.030$. The distance between the maximum damage point and the drill bit is indicated by the blue line.

For the ROP $V = 10$ m h^{-1}, as the damping ratio increases from 0.025 to 0.030, the maximum damage point of the drill string is located at $x_f = 6.6$ m above the drill bit, and the maximum cumulative damage decreases from $D = 0.62$ to $D = 0.10$. The maximum damage point of the drill string is located approximately $l_a/2$ above the drill bit.

From Eq. (23), it is noted that the cumulative fatigue damage is inversely proportional to the *m*-power of the damping ratio. When the damping ratio increases from 0.025 to 0.030, the maximum cumulative fatigue damage of the drill string is reduced by approximately 83.9%. If the damping ratio is increased slightly, the cumulative fatigue damage at each point of the drill string is reduced significantly. Therefore, a smaller damping ratio results in a higher risk of fatigue failure in the drill string. When performing sonic standing wave drilling in a formation with a low damping ratio, the dynamic stress in the drill pipe is extremely high, and it may even exceed the tensile strength of the drill string, resulting in the tensile fracture of the drill string.

To significantly reduce the dynamic stress in the sonic drill string when applied to shallow formations with low damping ratios, it is preferable to first employ travelling wave drilling and then sonic standing wave drilling, in order to prolong the service life of the sonic drill string.

3.4. Influence of drill pipe length on cumulative fatigue damage

During sonic drilling, the length of the drill string increases discontinuously, and the length of the drill pipe Δl affects the fatigue damage of the drill string. For the ROP $V = 10$ m h^{-1}

and damping ratio $\zeta = 0.025$, drill pipe lengths of $\Delta l = 0.5\ \mathrm{m}$, $\Delta l = 1\ \mathrm{m}$, and $\Delta l = 1.5\ \mathrm{m}$ are selected. Based on Eq. (23), the cumulative fatigue damage at each point in the drill string can be calculated. The curves of the cumulative damage at each point in the G105 drill pipe are plotted in Fig. 7.

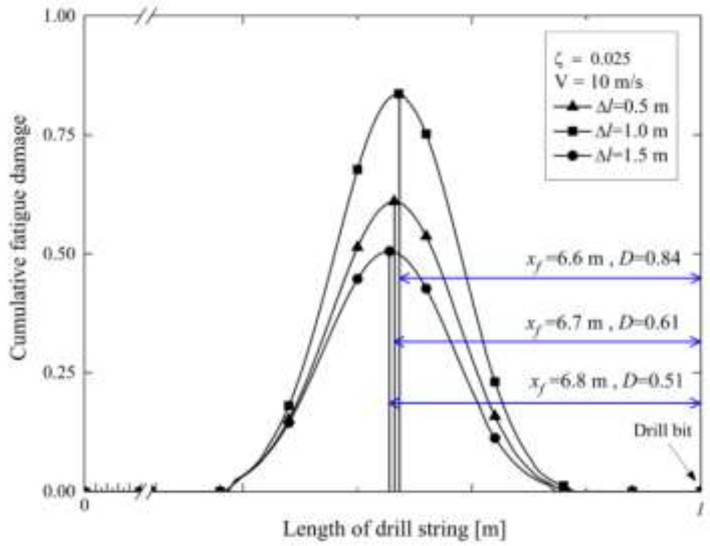

Fig. 7. Effect of the G105 drill pipe length on the fatigue damage in the drill string under the drilling conditions $V = 10\ \mathrm{m\ h^{-1}}$ and $\zeta = 0.025$.The three lines correspond to three drill pipe lengths: $\Delta l = 0.5\ \mathrm{m}$, $\Delta l = 1\ \mathrm{m}$, and $\Delta l = 1.5\ \mathrm{m}$. The distance between the maximum damage point and the drill bit is indicated by the blue line.

When the length of the drill pipe $\Delta l = 0.5\ \mathrm{m}$, the maximum damage point of the drill string is located at $x_f = 6.7\ \mathrm{m}$ above the drill bit, and the maximum damage value is $D = 0.61$. When the length of the drill pipe $\Delta l = 1\ \mathrm{m}$, the maximum damage point of the drill string is located at $x_f = 6.6\ \mathrm{m}$ above the drill bit, and the maximum damage value is $D = 0.84$. When the length of the drill pipe $\Delta l = 1.5\ \mathrm{m}$, the maximum damage point of the drill string is located at $x_f = 6.8\ \mathrm{m}$ above the drill bit, and the maximum damage value is $D = 0.51$. When drilling with different drill pipe lengths, the maximum damage point x_f of the drill string is located approximately $l_a/2$ above the drill bit, and it does not exceed l_a.

From Fig. 7, the cumulative damage at each point in the drill string is related to the selected length of the drill pipe. When using drill pipes of different lengths ($\Delta l = 0.5\ \mathrm{m}$, $\Delta l = 1\ \mathrm{m}$, and $\Delta l = 1.5\ \mathrm{m}$) with the same ROP and damping ratio, for each added drill pipe, the stress amplitude and the corresponding fatigue damage of the resonant standing wave at different drill string lengths can be obtained using Eqs. (20) and (23), respectively. Fig. 8 presents the maximum stress amplitude and maximum fatigue damage in the standing wave resonant drill string for different drill pipe lengths and corresponding lengths, with respect to the increasing drill string length.

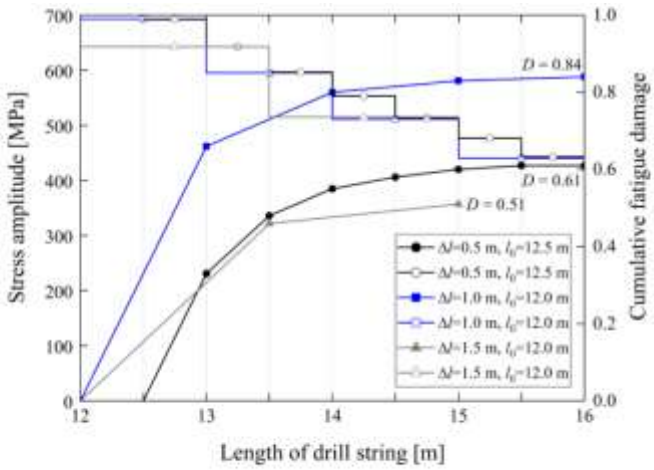

Fig. 8. Dynamic stress and fatigue damage for different drill pipe lengths of $\Delta l = 0.5$ m, $\Delta l = 1$ m, and $\Delta l = 1.5$ m under the drilling conditions of $V = 10$ m h^{-1} and $\zeta = 0.025$. The stress amplitude lines are plotted using the solid symbols, whereas the cumulative fatigue damage lines are plotted using the hollow symbols.

When the length of the drill pipe $\Delta l = 1$ m and the corresponding length $l_0 = 12$ m, with one drill pipe added (k =1), the length of the drill string satisfies $l_0 + \Delta l > l_a$. Accordingly, the maximum dynamic stress of the standing wave resonant drill string is $\sigma_{-1k} = 692.95$ MPa, and the fatigue damage at the point $x_f = 6.6$ m above the drill bit is $D_1 = 0.66$. When the drill pipe is connected in turn, the maximum dynamic stress decreases, and the fatigue damage at $x_f = 6.6$ m above the drill bit decreases to $D_2 = 0.14$, $D_3 = 0.03$, and $D_4 = 0.01$ for each additional drill pipe, respectively. The fatigue damage is reduced significantly. When the fifth drill pipe is added, there is no damage at $x_f = 6.6$ m, and the total fatigue damage is $D = 0.84$.

When the length of the drill pipe $\Delta l = 0.5$ m and the corresponding length $l_0 = 12.5$ m, with one drill pipe added (k =1), the drill string length satisfies $l_0 + \Delta l > l_a$. Accordingly, the standing wave resonant condition is available; the maximum dynamic stress of the drill string $\sigma_{-1k} = 692.95$ MPa, and the fatigue damage at the point $x_f = 6.7$ m above the drill bit is $D_1 = 0.33$. When the seventh drill pipe is added, the fatigue damage is

$D_7 = 0.00$, and the total fatigue damage at the point $x_f = 6.7$ m above the drill bit is $D = 0.61$.

When the length of the drill pipe $\Delta l = 1.5$ m and the corresponding length $l_0 = 12$ m, with one drill pipe added (k =1), the drill string length satisfies $l_0 + \Delta l > l_a$. Accordingly, the maximum dynamic stress of the standing wave resonant drill string is $\sigma_{-1k} = 642.72$ MPa, and the fatigue damage at the point $x_f = 6.8$ m above the drill bit is $D_1 = 0.46$. When the second drill pipe is added, the fatigue damage is $D_2 = 0.05$; when the third drill pipe is added, there is no damage at $x_f = 6.8$ m, and the total fatigue damage is $D = 0.51$.

From Fig. 8, when the length of the drill pipe is $\Delta l = 0.5$ m or $\Delta l = 1$ m, the drill string length of $l = 13$ m yields resonant standing waves. On comparing the length of the drill string in both cases, a longer standing wave drilling time with a smaller drill string length results in a greater amount of fatigue damage. For the drill pipe lengths of $\Delta l = 1$ m and $\Delta l = 1.5$ m, the lengths of the drill string are the same prior to the start of the resonant standing waves. However, when a 1.5 m drill pipe is added, the dynamic stress amplitude of the drill string decreases significantly, and the maximum fatigue damage is less than that with $\Delta l = 1$ m and $\Delta l = 1.5$ m.

Generally, different lengths of drill pipes lead to different dynamic stress amplitudes at each point of the drill string and different corresponding stress cycle times. The length of the drill pipe directly affects the number of stress cycles of the drill string under high stress and also affects the total fatigue damage of the drill string. Therefore, a reasonable choice of the drill pipe can help improve the service life of drill strings significantly.

3.5. Effect of sonic drill threaded connections on cumulative fatigue damage

Different thread forms and precision of threaded connections will affect the stress distribution and amplitude of sonic drill string. It is difficult to analytically solve the influence of threaded connections on the fatigue life of drill string. However, with the development of computer and finite element methods, it is easy to model the threaded connections, calculate the dynamic stress field, and determine that the dynamic stress amplitude σ_{-1k} at the threaded connection position x_j above the drill bit causes the maximum dynamic stress σ'_{-1k} due to the threaded connection stress concentration. The axial stress concentration factor (aSCF) of threaded connections can be written as $k_\sigma = \sigma'_{-1k} / \sigma_{-1k}$, in which the dynamic stresses are symmetrical cyclic stresses.

In this section, we simulate a specific threaded connection to demonstrate that the aSCF is constant. The model we adopted is the simplified API standard 5 thread/inch buttress thread joint. The geometric parameters are shown in Table 4 and material parameters G105 in Table1, respectively.

Table4. Dimension parameters of the model

Drill-string inner/outer diameter	External upset	Length: End of Pipe to Vanishing point	Shoulder length	Length: Transition between Shoulder and Pipe
Φ92.46/Φ114.3mm	3.27mm	92.39mm	30mm	110mm
Taper on diameter	Thread height	NO. of Threads per In.	Inclination of thread guide surface	Inclination of thread bearing surface
0.0625/1	1.57mm	5	10°	3°

Due to the small helix angle of the thread, the model is simplified to a 2D plane axisymmetric structure (the effect of the helix angle can be ignored). In this simulation, the linear quadrilateral CAX4R element is used. Set the contact type to Surface -surface contact, and set the contact surface coefficient of friction (CoF) is 0.02. Take the drill string with the length of 30 m as an example, select the drill pipe with the length of 1.5m, and the joint numbers are set from 1 to 19 in order of position from drill bit to sonic vibrator. The mesh, boundary diagram and stress nephogram of NO.6 joint are illustrated in Fig.9.

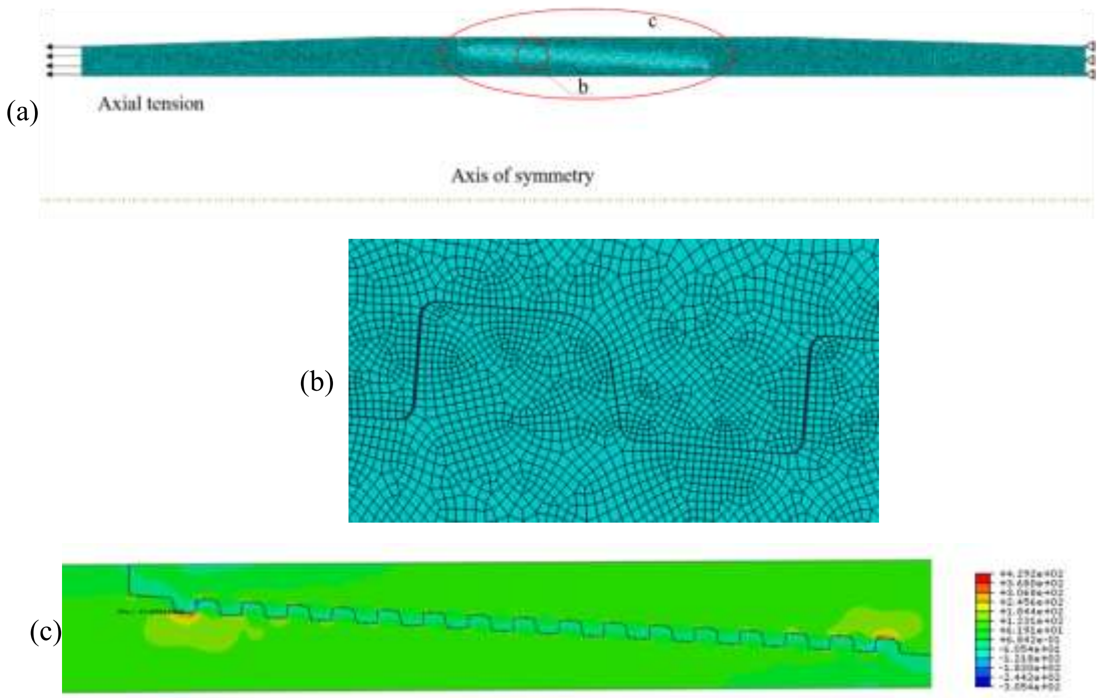

Fig. 9. Mesh and boundary of the FE model: (a) Schematic diagram of the 2D axisymmetric model boundary, the left end is the load boundary, and the right end only limits the axial displacement (axial

displacement U2=0). (b) Detailed mesh around thread root. The global mesh size is 1mm, and a finer mesh with seed size 0.1mm was used in the threads of the model. (c) Nephogram of axial stress field at the 6th threaded joint, the applied axial stress is calculated as 105.22MPa by Eq. (20)

The stress nephograms of joints at each position are similar, and the maximum stress is generated at the root of the first buckle or the last buckle of the connection.

Eq. (20) is used to calculate the fatigue stress amplitude σ_{-1k} at different connections. By applying the amplitude to the model load boundary, the maximum stress of connection at the different positions can be obtained, so that the aSCF can be calculated by $k_\sigma = \sigma'_{-1k} / \sigma_{-1k}$. The calculation results of aSCF at different joints are shown in Table 5:

Table 5. Calculated aSCF of threaded joints at different positions (CoF=0.02)

Joint number	Distance from joint to the bit x_j (m)	Load stress amplitude σ_{-1k} (MPa)	Maximum stress of threaded connection σ'_{-1k} (MPa)	Calculated aSCF $k_\sigma = \sigma'_{-1k} / \sigma_{-1k}$
2	3	40.18	164.5	4.09
4	6	76.43	312.1	4.08
6	9	105.22	429.2	4.08
8	12	123.72	504.5	4.08
10	15	130.13	530.5	4.08
12	18	123.81	504.9	4.08
14	21	105.36	429.8	4.08
16	24	76.58	312.7	4.08
18	27	40.25	164.7	4.09

It can be seen from Table5 that the aSCF in the elastic range can be treated as a constant within the error range.

Because k_σ is a constant, for any joint with given parameters, the maximum stress of the connection at any position can be calculated by $\sigma'_{-1k}=k_\sigma\sigma_{-1k}$, so that the program in Fig. 4 can be used to realize the theoretical calculation of the connection fatigue damage.

Different from calculating the fatigue damage at the non-joint drill string, due to the introduction of aSCF k_σ at the threaded connection, the expressions of σ'_{-1k} and the upper limit l_b' of the drill string length causing fatigue damage are changed. According to Eqs. (16) and (20), Eqs. (16a) and (20a) can be obtained.

$$l_b' = \sqrt{\frac{k_\sigma \pi r m_e}{\zeta \sigma_{-1} S}} \cdot \sqrt{\frac{E}{\rho}} \tag{16a}$$

$$\sigma'_{-1k} = k_\sigma \sigma_{-1k} = \frac{k_\sigma}{\zeta} \cdot \frac{\pi r E m_e}{\rho S (l_0 + k\Delta l)^2} \sin\left(\frac{\pi \cdot x_j}{l_0 + k\Delta l}\right) \tag{20a}$$

Due to the change of σ'_{-1k} and l_b', the total number of stress cycles N_k' corresponding to σ'_{-1k} at threaded connection x_j can be obtained from Eq. (2) as Eq. (21a).

$$N_k' = \left(\frac{\sigma_{-1}}{\sigma'_{-1k}}\right)^m N_c = \left(\frac{\sigma_{-1}}{k_\sigma \sigma_{-1k}}\right)^m N_c \tag{21a}$$

Considering the influence of aSCF, the cumulative fatigue damage of threaded connections can be expressed as Eq. (23a).

$$D' = \sum \frac{n_k}{N_k'} = \frac{{k_\sigma}^m \pi^m r^{m+1}}{2N_C(\sigma_{-1})^m} \cdot \left(\sqrt{\frac{E}{\rho}}\right)^{2m+1} \cdot \left(\frac{m_e}{S}\right)^m \cdot \frac{1}{V\zeta^m} \cdot \sum_{k=1}^{k'_{\max}} \left[\frac{\Delta l}{(l_0 + k\Delta l)^{2m+1}} \cdot \sin^m\left(\frac{\pi \cdot x_j}{l_0 + k\Delta l}\right)\right] \tag{23a}$$

It can be seen from Eqs (16a) and (23a) that aSCF k_σ increases the upper limit of the drill string damage length l_b' and the cumulative fatigue damage of threaded connections D'.

The fatigue damage of any connection under the standing wave vibration can be calculated by using Eq.(23a). aSCF k_σ of the drill pipe connections significantly reduces the fatigue life of the drill string.

4. Conclusions

In this study, through the modelling and analysis of the standing wave vibrations in variable-length drill strings excited by a sonic vibrator, based on one-dimensional wave theory and the Palmgren–Miner fatigue damage rule, the theoretical formulation of the cumulative fatigue damage in variable-length drill strings is established innovatively. The following conclusions can be drawn:

1. The fatigue damage of the sonic drill string is closely related to the technical parameters of the system and drill pipe. Adopting a drill pipe material with a high fatigue limit, reducing the total static moment m_e, increasing the cross-sectional area S, and selecting the appropriate length of the drill pipe to avoid high stress damage areas are all conducive methods to reduce the fatigue damage in drill strings.

2. The construction parameters (i.e. rate of penetration V and formation damping ratio ζ) also affect the fatigue damage of the drill string, and the damage is more sensitive to the formation damping ratio. Slightly reducing the damping ratio significantly increases the cumulative fatigue damage of the drill string. Reducing the drilling time in a shallow hole under high stress levels is, therefore, beneficial in decreasing the total fatigue damage of the drill

string.

3. The starting oscillation length of standing wave resonant drilling l_a in a shallow hole is determined by the upper frequency limit of the sonic vibrator; the dynamic stress level in the drill string decreases rapidly as the borehole is extended. Throughout the first-order standing wave resonant drilling, the maximum fatigue damage point x_f in the drill string is located approximately $l_a/2$ above the drill bit, and it does not exceed l_a and is unrelated to the length of the drill string corresponding to the drilling depth.

Research on the fatigue damage of sonic drill strings can help guide sonic drill designs and practices for improving the service life of drilling tools; it can also help reduce the occurrence of drilling-related accidents. Moreover, this study promotes the theoretical understanding and exploration of stable/variable-length standing wave oscillators.

Credit authorship contribution statement

Changgen Bu: Conceptualization, Methodology, Formal analysis, Writing - Reviewing and Editing, Funding acquisition. **Jing Xiao:** Software, Investigation, Writing - Original Draft, Visualization. **Shengyu He:** Software, Visualization, Writing - Reviewing and Editing. **Marian Wiercigroch:** Writing - Reviewing and Editing.

Acknowledgments

This work was supported by the National Natural Science Foundation of China (Grant NO.51775523). The authors would like to thank Mr. Ali Hassanirad for his suggestions on FEA of drill pipe joint.

References

Albdiry, M.T., Almensory, M.F., 2016. Failure analysis of drillstring in petroleum industry: A review. Eng. Fail. Anal. 65, 74-85.

Baek, S.H., Cho,S.S., Joo ,W.S., 2008. Fatigue life prediction based on the rainflow cycle counting method for the end beam of a freight car bogie. Int. J. Automot. Technol. 9(1), 95-101.

Barrow, J.C., 1994. The Resonant Sonic Drilling Method: An Innovative Technology for Environmental Restoration Programs. Ground. Water. Monit. R. 14(2), 153-160.

Benkabouche, S., Guechichi,H., Amrouche, A., Benkhettab ,M., 2015. A modified nonlinear fatigue damage accumulation model under multiaxial variable amplitude loading. Int. J. Mech. Sci. 100,180-194.

Bertini,L., Beghini, M., Santus, C., Baryshnikov ,A., 2008. Resonant test rigs for fatigue full scale testing of oil drill string connections. Int. J. Fatigue.30(6),978-988.

Bu,C.G., Sun ,L., Hu, Y.B., Xia, B.R., 2015. Research on flexible drill string vibration induced by sonic harmonic excitation. Trans. Can. Soc. Mech. Eng.39(2),281-291.

Chen,H., Chen, Y., Yang ,Y., 2014. A fatigue and low-energy shock-based approach to predict fatigue life. J. Mech. Sci. Technol. 28(10), 3977-3984.

Chen,W. C., 1990. Drillstring Fatigue Performance. SPE. Drill. Eng. 5 (2), 129–134.

Ciavarella, M., Dantuono, P., Demelio, G.P., 2017. A simple finding on variable amplitude (Gassner) fatigue SN curves obtained using Miner's rule for unnotched or notched specimen. Eng. Fract. Mech.176, 178-185.

Corten, H.T., Dolan, T.J., 1956. Cumulative fatigue damage. Proceedings of International conference on fatigue of metals, IME and ASME, London: IME.1,235.

Dao, N.H., Sellami, H., 2012. Stress intensity factors and fatigue growth of a surface crack in a drill pipe during rotary drilling operation. Eng. Fract. Mech. 96, 626-640.

Fatemi, A., Yang, L., 1998. Cumulative fatigue damage and life prediction theories: a survey of the state of the art for homogeneous materials. Int. J. Fatigue. 20(1), 9-34.

Fitzka, M., Mayer, H., 2016. Constant and variable amplitude fatigue testing of aluminum alloy 2024-T351 with ultrasonic and servo-hydraulic equipment. Int. J. Fatigue. 91, 363-372.

Forman, R.G., Kearney, V.E., Engle, R.M., 1967. Numerical analysis of crack propagation in cyclic-loaded structures. J. Basic. Eng. 89(3), 459-463.

Freitas, M.D., 2017. Multiaxial fatigue: From materials testing to life prediction. Theor. Appl. Fract. Mech. 92, 360-372.

Ghasemloonia, A., Rideout, D. G., Butt, S. D., 2015. A review of drillstring vibration modeling and suppression methods. J. Petrol. Sci. Eng. 131, 150-164.

Grondin, G. Y., Kulak, G. L., 1994. Fatigue Testing of Drillpipe. SPE. Drill. Completion. 9(2), 95-102.

He, H., Liu, H., Zhu, C., Wei, P.T., Sun, Z.D., 2018. Study of rolling contact fatigue behavior of a wind turbine gear based on damage-coupled elastic-plastic model. Int. J. Mech. Sci. 141, 512-519.

ISO11961:2008(IDT), Petrolem and natural gas industries--steel drill pipe. Washington. DC, 2005.

Jansen, J. D.,1991. Non-Linear Rotor Dynamics as Applied to Oilwell Drillstring Vibrations. J. Sound. Vib.147 (1), 115–135.

Jiang, G.C., Sun, J.S., He, Y.B., Cui, K.X., Dong, T.F., Yang, L.L., Yang, X.K., Wang, X.X., et al., 2021. Novel water-based drilling and completion fluid technology to improve wellbore quality during drilling and protect unconventional reservoirs. Engineering. 2021.

Jiao, R., He, X.F., Li, Y.H., 2018. Individual aircraft life monitoring: An engineering approach for fatigue damage evaluation. Chinese. J. Aeronaut. 31(4), 727-739.

Kapitaniak, M., Hamaneh, V. V., Chávez, J.P., Nandakumar, K., Wiercigroch, M., 2015. Unveiling Complexity of Drill-String Vibrations: Experiments and Modelling. Int. J. Mech. Sci. 101-102,324-337.

Knight, M. J., Brennan, F. P., 1999. Fatigue life improvement of drill collars through control of bore eccentricity. Eng. Fail. Anal. 6(5), 301-319.

Leine, R., Campen, D., Kraker, A., Steen, L., 1998. Stick slip vibrations induced by alternate friction models. Nonlinear. Dynam. 16(1), 41-54.

Liao, C. M., Vlajic, N., Karki, H., Balachandran, B., 2012. Parametric studies on drill-string motions. Int. J. Mech. Sci. 54(1), 260-268.

Lin, T., Zhang, Q., Lian, Z., Liu, Y.G., Zhang, Y., Chen, Y., 2016. Multi-axial fatigue life prediction of drill collar thread in gas drilling. Eng. Fail. Anal. 59, 151-160.

Lin, Y.H., Li, G.H., Hu, Q., Liu, W.Y., 2015. Experimental Study on Drill Pipes Stress-Fatigue Life Curve. Petrol. Drill. Tech. 43(4), 124-128. Chinese.

Liu, F., Zhou, S.M., Xia, C.Y., Zeng, D.Z., Shi, T.H., 2016. Optimization of fatigue life distribution model and establishment of probabilistic S–N curves for a 165 ksi grade super high strength drill pipe steel. J. Petrol. Sci. Eng. 145, 527-532.

Liu, X.B.，Vlajic, N., Long, X.H., Meng, G., Balachandran, B., 2014. State-Dependent Delay Influenced Drill-String Oscillations and Stability Analysis. J. Vib. Acoust. 136(5), 051008.

Lv, Z.Q., Huang, H.Z., Zhu, S.P., Gao, H.Y., Zuo, F.J., 2015. A modified nonlinear fatigue damage accumulation model. Int. J. Damage. Mech. 24(2), 168-181.

Macdonald, K. A., Bjune, J. V., 2007. Failure analysis of drillstrings. Eng. Fail. Anal. 14(8), 1641-1666.

Manson, S.S., 1966. Interfaces between fatigue creep and fracture. Int. J. Fracture. 2(1), 327-363.

Mayer, H., Schuller, R., Fitzka, M., 2013. Fatigue of 2024-T351 aluminum alloy at different load ratios up to 1010 cycles. Int. J. Fatigue. 57, 113-119.

Mihajlović, N., Wouw, N.v.d., Rosielle, P.C.J.N., Nijmeijer, H., 2007. Interaction Between Torsional and Lateral Vibrations in Flexible Rotor Systems With Discontinuous Friction. Nonlinear. Dynam. 50 (3), 679–699.
Miner, M.A.,1945. Cumulative fatigue in damage. J. Appl. Mech.12(3), 159-64.
Moradi, S., Ranjbar, K., 2009. Experimental and computational failure analysis of drillstrings. Eng. Fail. Anal. 16(3), 923-933.
Nesládek, M., Paniel, M., Jurenka, J., Rika, J., Kuelka, J., 2012. Fretting fatigue - Experimental and numerical approaches. Int. J. Fatigue. 44, 61-73.
Ojanomare, C., Cornetti, P., Romagnoli, R., Surace, C., 2017. Fatigue crack growth analysis of drill pipes during rotary drilling operations by the multiple reference state weight function approach. Eng. Fail. Anal. 74,11-34.
Paris, P., Erdogan, F., 1963. Critical Analysis of Crack Propagation Laws. J. Basic. Eng. 85(4), 528-533.
Proso, U., Slavi, J., Boltear, M., 2016. Vibration-fatigue damage accumulation for structural dynamics with non-linearities. Int. J. Mech. Sci. 106, 72-77.
Rahman, M.K., Hossain, M.M., Rahman, S.S.,1999. Stress concentration incorporated fatigue analysis of die-marked drill pipes. Int. J. Fatigue. 21(8), 799-811.
Rao, J., Pathak, A., Chawla, A., 2001. Blade life: a comparison by cumulative damage theories. J. Eng. Gas. Turb. Power. 123(4), 886–892.
Santus, C., Bertini, L., Burchianti, A., Inoue, T., Sakurai, N., 2018. Fatigue resonant tests on drill collar rotary shouldered connections and critical thread root identification. Eng. Fail. Anal. 89, 138-149.
Santus, C., 2008. Fretting fatigue of aluminum alloy in contact with steel in oil drill pipe connections, modeling to interpret test results. Int. J. Fatigue. 30(4), 677-688.
Shi, R.M., 2012, Aircraft structural vibration design and testing. Beijing: Aviation Industry Press; Chinese.
Sikal, A., Boulet, J.G., Menand, S., Sellami, H., 2008. Drill Pipe Stress and Cumulative Fatigue Analysis in Complex Wells Drilling: New Approach in Fatigue Optimization.In: SPE Annual Technical Conference and Exhibition.
Sun, L., Bu, C.G., Hu, P.D., Xia, B.R., 2017. The Transient Impact of the Resonant Flexible Drill String of a Sonic Drill on Rock. Int. J. Mech. Sci. 122, 29-36.
Sun, Q., Dui, H.N., Fan, X.L., 2014. A statistically consistent fatigue damage model based on Miner's rule. Int. J. Fatigue. 69,16-21.
Sun, S., Li, L., He, K., Yue, Z.F., Yang, W.Z., Yu, Z.Y., 2020. Fretting fatigue damage mechanism of Nickel-based single crystal superalloys at high temperature. Int. J. Mech. Sci. 186, 105894.
Susmel, L., Tovo, R., Lazzarin, P., 2005. The mean stress effect on the high-cycle fatigue strength from a multiaxial fatigue point of view. Int. J. Fatigue. 27(8), 928–943.
Vandiver, K. J., Nicholson, W. J., Shyu, R. J., 1990. Case Studies of the Bending Vibration and Whirling Motion of Drill Collars. SPE. Drill. Eng. 5(4), 282–290.
Walker, K.,1970. The Effect of Stress Ratio During Crack Propagation and Fatigue for 2024-T3 and 7075-T6 Aluminum. In: STP462-EB Effects of Environment and Complex Load History on Fatigue Life. p. 1-14.
Wang, Z.H., Liu, X.Y., Zhang, H.Q., Wang, Y., Xu, Y.F., Peng, B.L., Liu, Y., 2022. Modeling of kinetic characteristics of alkaline-surfactant-polymer-strengthened foams decay under ultrasonic standing wave. Petrol. Sci. 19(4), 1825-1839.
Wen, B.C., 2009. Theory of mechanical vibration and its applications. Beijing: Higher Education Press. p. 134-36. Chinese.
Xia, T.X., Yao, W.X., 2013. Comparative research on the accumulative damage rules under multiaxial block loading spectrum for 2024-T4 aluminum alloy. Int. J. Fatigue. 48, 257-265.
Xiao, J., Bu, C.G., Hu, Y.B., He, S.Y., 2020. Influence of sonic vibrator mass on the modal frequency of drill string. Trans. Can. Soc. Mech. Eng. 44(1), 65-71.
Xu, L., Wang, K., Yang, X.B., Su, Y.Y., Yang, J.W., Liao, Y.Z., et al., 2021. Model-driven fatigue crack characterization and growth prediction: A two-step, 3-D fatigue damage modeling framework for structural health monitoring. Int. J. Mech. Sci.195, 106226.
Yigit, A. S., Christoforou, A.P., 2006. Stick-Slip and Bit-Bounce Interaction in Oil-Well Drillstrings. J. Energy. Resour. Technol. 128 (4), 268–274.
Zamani, S. M., Hassanzadeh-Tabrizi, S. A., Sharifi, H., 2016. Failure analysis of drill pipe: A review. Eng. Fail. Anal. 59, 605-623.
Zambrano, A., Foti, D., 2014. Damage indices evaluation for seismic resistant structures subjected to low-cycle fatigue phenomena. Int. J. Mech. Sci. 78, 106-117.
Zhang, Q., Hu, X., Zhang, Z., Sun, T., Wu, J.W., Li, Y.F., et al., 2021. The mean stress and phase angle effect on multiaxial fatigue behavior of a TiAl alloy: Failure analysis and life modeling. Int. J. Mech. Sci. 193,106123.
Zhao, B., Xie, L., Song, J., Ren, J.G., Wang, B.W., Zhang, S.J., 2020. Fatigue life prediction of aero-engine compressor disk based on a new stress field intensity approach. Int. J. Mech. Sci. 165,105190.
Zhao, D., Hovda, S., Sangesland, S., 2018. Whirl Simulation of Drill Collar and Estimation of Cumulative Fatigue Damage on Drill-Collar Connection. SPE. J. 23(2), 286-300.
Zhao, S.B., 2000. Study on the accuracy of fatigue life predictions by the generally used damage accumulation theory. J. Mech. Strength. 22(3), 206–209. Chinese.
Zhu, S.P., Huang, H.Z., Liu, Y., He, L.P., Liao, Q., 2012. A Practical Method for Determining the Corten-Dolan Exponent and Its Application to Fatigue Life Prediction. Int. J. Turbo. Jet. Eng. 29(2),79-87.
Zhu, S.P., Huang, H.Z., Wang, Z.L., 2011. Fatigue Life Estimation Considering Damaging and Strengthening of Low amplitude Loads under Different Load Sequences Using Fuzzy Sets Approach. Int. J. Mech. Sci. 20(6), 876-899.
Zhuang, X.A., Ma, Y.A., Zhao, Z., 2019. Fracture prediction under nonproportional loadings by considering

combined hardening and fatigue-rule-based damage accumulation. Int. J. Mech. Sci. 150,51-65.